

# Low-dose laulimalide represents a novel molecular probe for investigating microtubule organization

Melissa J. Bennett,<sup>1</sup> Gordon K. Chan,<sup>2</sup> J.B. Rattner<sup>1,3</sup> and David C. Schriemer<sup>1,\*</sup>

<sup>1</sup>Department of Biochemistry and Molecular Biology; University of Calgary; Calgary, Alberta, Canada; <sup>2</sup>Department of Oncology; University of Alberta; Cross Cancer Institute; Edmonton, AB Canada; <sup>3</sup>Department of Anatomy and Cell Biology; University of Calgary; Calgary, AB Canada

**Keywords:** laulimalide, centrosome, spindle pole, microtubules, kinetochore tension

Laulimalide is a natural product that has strong taxoid-like properties but binds to a distinct site on  $\beta$ -tubulin in the microtubule (MT) lattice. At elevated concentrations, it generates MTs that are resistant to depolymerization, and it induces a conformational state indistinguishable from taxoid-treated MTs. In this study, we describe the effect of low-dose laulimalide on various stages of the cell cycle and compare these effects to docetaxel as a representative of taxoid stabilizers. No evidence of MT bundling in interphase was observed with laulimalide, in spite of the fact that MTs are stabilized at low dose. Cells treated with laulimalide enter mitosis but arrest at prometaphase by generating multiple asters that coalesce into supernumerary poles and interfere with the integrity of the metaphase plate. Cells with a preformed bipolar spindle exist under heightened tension under laulimalide treatment, and chromosomes rapidly shear from the plate, even though the bipolar spindle is well-preserved. Docetaxel generates a similar phenotype for HeLa cells entering mitosis, but when treated at metaphase, cells undergo chromosomal fragmentation and demonstrate reduced centromere dynamics, as expected for a taxoid. Our results suggest that laulimalide represents a new class of molecular probe for investigating MT-mediated events, such as kinetochore-MT interactions, which may reflect the location of the ligand binding site within the interprotofilament groove.

## Introduction

Until recently, the taxol binding domain in the lumen of the microtubule (MT) represented the only known site for inducing microtubule stabilization with small molecules. However, a structural study using the polyketide laulimalide has revealed a second MT-stabilizing site and thus, potentially, a fourth distinct druggable site in  $\alpha/\beta$  tubulin.<sup>1</sup> The site is situated on the exterior of the MT on  $\beta$ -tubulin near the charged C-terminal tail, which was recently validated with the aid of macrolide-resistant cell lines.<sup>2,3</sup> Laulimalide exhibits microtubule-stabilizing activity and presents new opportunities for the development of antimitotic therapies.<sup>4</sup> It is highly cytotoxic, inhibiting cell proliferation in numerous cancer cell lines at low nM IC<sub>50</sub> values.<sup>4,5</sup> It is also active in multidrug-resistant cancer cell lines overexpressing P-glycoprotein (P-gp) and is both effective in taxoid-resistant cell lines<sup>5</sup> and synergistic with taxoids.<sup>6</sup> These findings suggest that laulimalide may form the basis for a next-generation antimitotic agent, although we note lingering concerns over toxicity.<sup>7</sup>

MT stabilizers interfere with MT dynamics and alter mitotic processes.<sup>8,9</sup> This has made taxoids a useful set of probes for dissecting aspects of mitotic behavior such as kinetochore tension, spindle checkpoint activation, separation of centrosomes and

mitotic slippage.<sup>10-15</sup> An agent that induces MT stabilization by engaging a unique site may provide new ways to study mitotic properties. Before laulimalide and the site that it occupies can be exploited for therapeutics or molecular probes, a more extensive investigation of cellular phenotype and mode of action is required. In early efforts applied to asynchronous cultures, cells were noted to arrest at G<sub>2</sub>/M and form circular or multipolar spindles with multiple centrosomes organized into a circular arrangement, bearing spindle MTs radiating outwards.<sup>4,7,16</sup> The formation of supernumerary spindle poles was suggested to arise from centrosome/centriole amplification,<sup>16</sup> and the formation of multiple micronuclei was noted.<sup>4</sup>

The cellular phenotype and mechanism of cell death induced by MT stabilizers is dependent on drug concentration and length of treatment.<sup>17,18</sup> The use of laulimalide at elevated concentrations and/or long treatment times in the initial studies suggested a complex phenotype arising from primary and secondary events. In this study, we establish a reduced laulimalide concentration required to induce saturable effects in mitosis under short time exposures. These conditions were used to investigate the effect of laulimalide in other stages of the cell cycle using real-time imaging, indirect immunofluorescence (IIF) and electron microscopy on both synchronous and asynchronous cell populations. These

\*Correspondence to: David C. Schriemer; Email: dschriem@ucalgary.ca  
Submitted: 05/07/12; Revised: 06/21/12; Accepted: 07/28/12  
<http://dx.doi.org/10.4161/cc.21411>

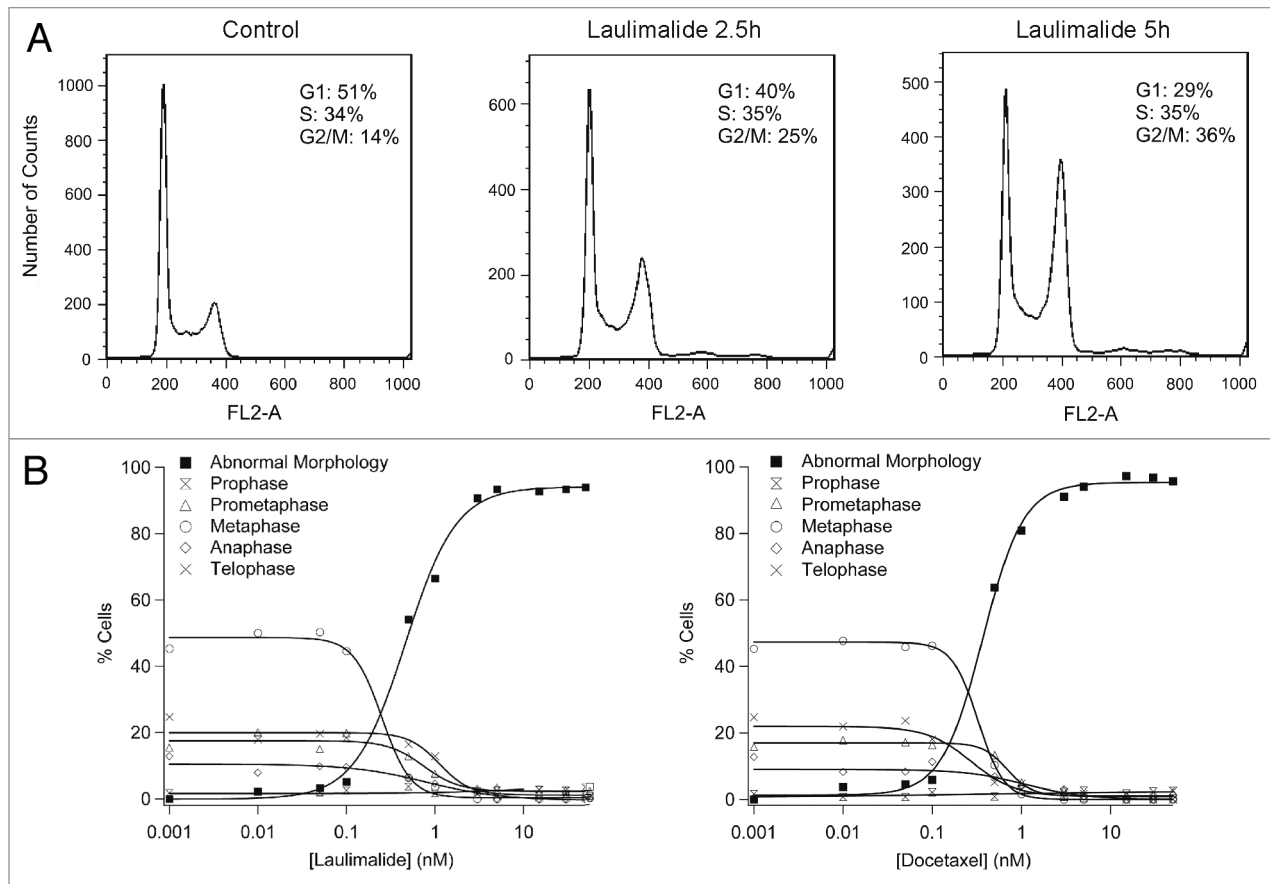


**Figure 1.** Laulimalide treatment leads to accumulation of HeLa cells in mitosis with an aberrant phenotype. (A) Cell cycle analysis by flow cytometry after treatment with a DMSO control (left panel), 30 nM laulimalide for 2.5 h (middle panel) and 30 nM laulimalide for 5 h (right panel). Cells progress through interphase and accumulate in G<sub>2</sub>/M. (B) Dose-response plots quantitating the spindle perturbation phenotype for mitotic cells treated with 0–50 nM of laulimalide (left) or docetaxel (right) for 2.5 h, using immunofluorescence analysis with M4491,  $\beta$ -tubulin antibody and DAPI.

results are compared with the microtubule stabilizer docetaxel, a taxoid with well-characterized cellular effects,<sup>18–20</sup> in an attempt to uncouple the fundamental property of MT stabilization, which laulimalide and docetaxel hold in common, from the site of stabilization, where the two drugs differ.<sup>1</sup> In this paper we show that laulimalide represents a class of MT stabilizer that is distinct from the taxoids, inducing notable differences in cellular phenotype relative to docetaxel throughout the cell cycle, with the exception of prophase/prometaphase. Our findings provide a foundation for future mechanistic studies toward the role of MT binding site in regulating the mitotic spindle and point to the utility of laulimalide as a unique molecular probe for the interprotofilament region of the MT.

## Results

**Dose-response analysis.** As MT stabilizers are known for their ability to arrest cells in G<sub>2</sub>/M,<sup>9</sup> we decided to determine the optimal concentration for further studies from a dose-response analysis of mitotic progression. Treatment duration was chosen to allow sufficient time to fully encompass mitosis and emphasize the primary effects of laulimalide. Asynchronous HeLa cells were treated with 0–50 nM laulimalide and analyzed using indirect

immunofluorescence. HeLa cells were chosen for this study because of their long history of use in characterizing other MT stabilizers, and because they demonstrate normal mitotic spindle assembly and a robust mitotic checkpoint.<sup>18,21–24</sup>

To confirm that laulimalide induces the accumulation of cells in mitosis at low doses, we first measured the mitotic index in comparison to a control with just the vehicle (DMSO). The mitotic index for the control cells was 9.6% (24 out of 250 cells). In the presence of 1 nM laulimalide and 30 nM laulimalide, the mitotic index increased to 13% and 19%, respectively, when cells were treated for 2.5 h. Flow cytometry was then performed on asynchronous cells treated with 30 nM laulimalide for 2.5 and for 5 h, relative to the control. Laulimalide induced a noticeable time-dependent accumulation of cells in G<sub>2</sub>/M, but cells otherwise progressed through interphase (Fig. 1A). We then determined if laulimalide influenced mitotic morphology at the 2.5 h exposure. Mitotic cells (n = 100) at each dose were examined and categorized according to mitotic stage and their spindle/chromosome pattern and plotted as a dose-response curve relative to a similar analysis of docetaxel (Fig. 1B). Cells were considered to have an abnormal morphology if they contained an aberrant chromosome pattern and/or more than two microtubule asters. From the abnormal cells, EC<sub>50</sub> values of 0.38 nM were obtained

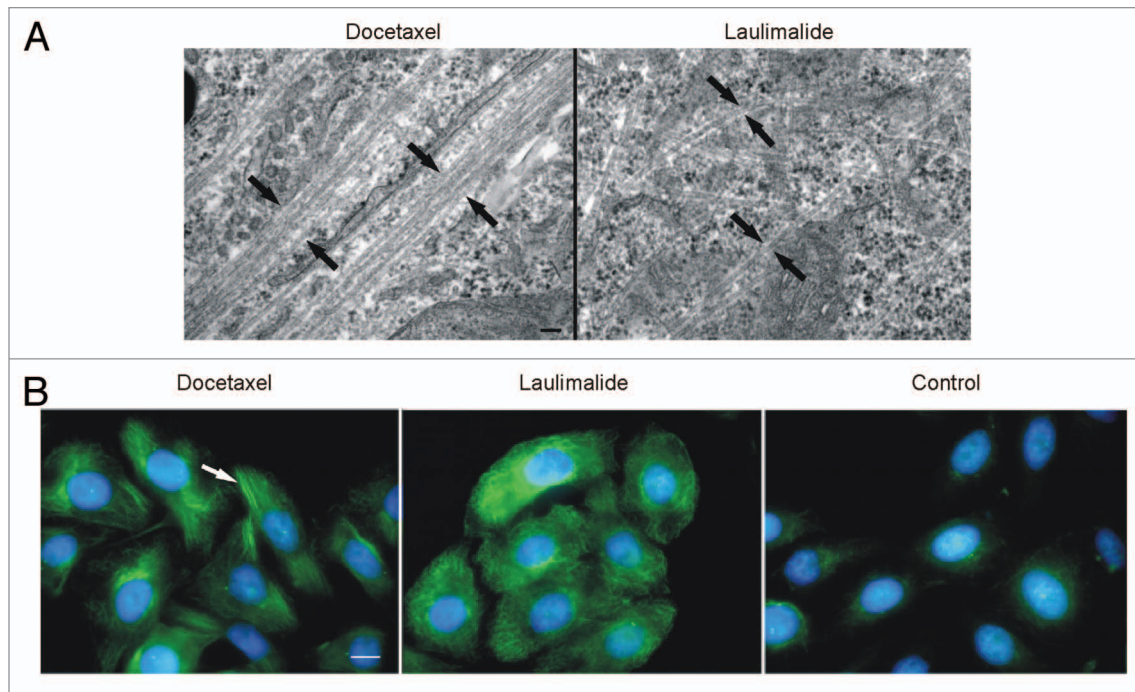


**Figure 2.** Laulimalide stabilizes but does not bundle HeLa cell microtubules in interphase. (A) Electron micrograph of interphase HeLa cells treated with 30 nM docetaxel and 30 nM laulimalide for 2.5 h. Microtubule bundling is evident upon docetaxel treatment but not upon laulimalide treatment (black arrows). Scale bar represents 100 nm. (B) Immunofluorescence of acetylated tubulin in cells treated with DMSO, 30 nM laulimalide and 30 nM docetaxel for 2.5 h. Tubulin shown in green and DAPI in blue, and the white arrow indicates microtubule bundling. Scale bar represents 10  $\mu$ m.

for laulimalide and 0.49 nM for docetaxel. At this level of analysis, we note the apparent similarity between these two drugs. We used docetaxel (a paclitaxel analog) in this study, as our previous work showed that laulimalide and docetaxel generate MTs indistinguishable in stability and conformation, permitting differences in cellular phenotype to be attributed to different binding sites instead of allosteric effects.<sup>1</sup> We selected 30 nM as the concentration for further experiments, because it provided a stable “abnormal” mitotic effect in both cases, and a 2.5 h exposure was used during the analysis of successive stages of the cell cycle (interphase, prophase/prometaphase and metaphase), except where noted, to emphasize primary effects of drug treatment.

**Effect of laulimalide on interphase MT populations.** Having optimized treatment conditions for mitotic cells, we then determined how this concentration altered MT properties in the interphase cell. MT stabilizers of the taxoid class have been shown to induce MT bundling in interphase,<sup>21</sup> and so has laulimalide at high concentrations.<sup>4,16</sup> However, laulimalide-treated cells showed no evidence of bundling at the dose optimized for mitotic defects, which is clear when comparing electron micrographs of cells treated with either drug (Fig. 2A). We then tested if MT stability is maintained at this dose by exploring tubulin acetylation as a surrogate for the stable state. MT stabilization correlates with increased microtubule posttranslational modifications, such as acetylation.<sup>25,26</sup> We found that vehicle-treated control cells demonstrated very little evidence of acetylation; however, both drugs induced extensive tubulin acetylation, and staining revealed morphologies in keeping with the bundling status (Fig. 2B). That is, the acetylation pattern is predominantly seen on microtubule

bundles in the docetaxel-treated cells and on the unbundled microtubules in the laulimalide-treated cells (Fig. 2B). There does not appear to be a direct correlation between acetylation and microtubule bundling therefore, but we may interpret the increased acetylation as evidence of stabilized microtubules (or at the very least, that acetylation is independent of the stabilizing ligand used).

**Effect of laulimalide on early mitosis.** After establishing that laulimalide-treated HeLa cells progress through interphase, we examined the behavior of laulimalide-treated cells as they entered mitosis. Live-cell imaging was performed on mCherry GFP-histone-H2B HeLa cells synchronized at G<sub>1</sub>/S using a double thymidine block, released for 8 h followed by the addition of laulimalide. Cells entered mitosis and then proceeded through prophase and nuclear envelope breakdown. This was followed by the formation of multiple MT asters encompassed by circular chromosomal arrays (Fig. 3). Similar results were obtained during live-cell imaging of cells treated with docetaxel, and these were confirmed with electron microscopy of drug-treated prometaphase cells (Fig. S1). Therefore, HeLa cells treated with either laulimalide or docetaxel clearly enter mitosis, but treatment prevents the formation of a proper bipolar spindle.

To investigate the transition from interphase to mitosis in greater detail, HeLa cells were first synchronized in G<sub>2</sub>/M, then treated with drug and analyzed using IIF. During prophase, the interphase microtubule array disassembled, and then a population of MTs was detected around the nucleus. Cells in early prometaphase displayed numerous MT asters arrayed along the nuclear and plasma membranes (Fig. 4A). In the absence of

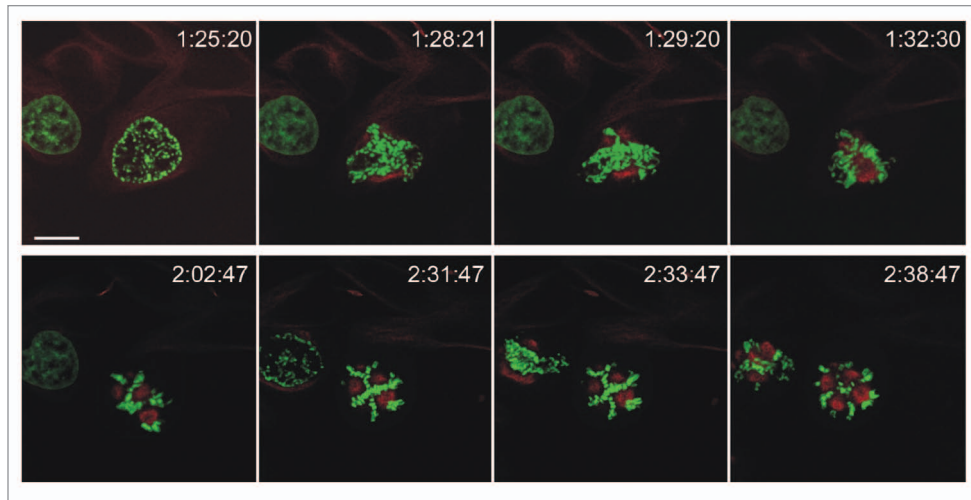


**Figure 3.** Laulimalide treatment does not prevent entry into mitosis. Time-lapse images from  $G_2/M$  phase, using mCherry tubulin and GFP-histone-H2B HeLa cells treated with 30 nM laulimalide, synchronized at  $G_2/M$  using a double thymidine block as described in the text. Cells clearly enter prophase and repartition interphase tubulin into an aberrant multipolar structure with circularly-distributed chromosomal arrays. Times in hours:minutes:seconds indicate the period of incubation in laulimalide. Tubulin is shown in red and histone H2B in green. Scale bar represents 13  $\mu\text{m}$ .

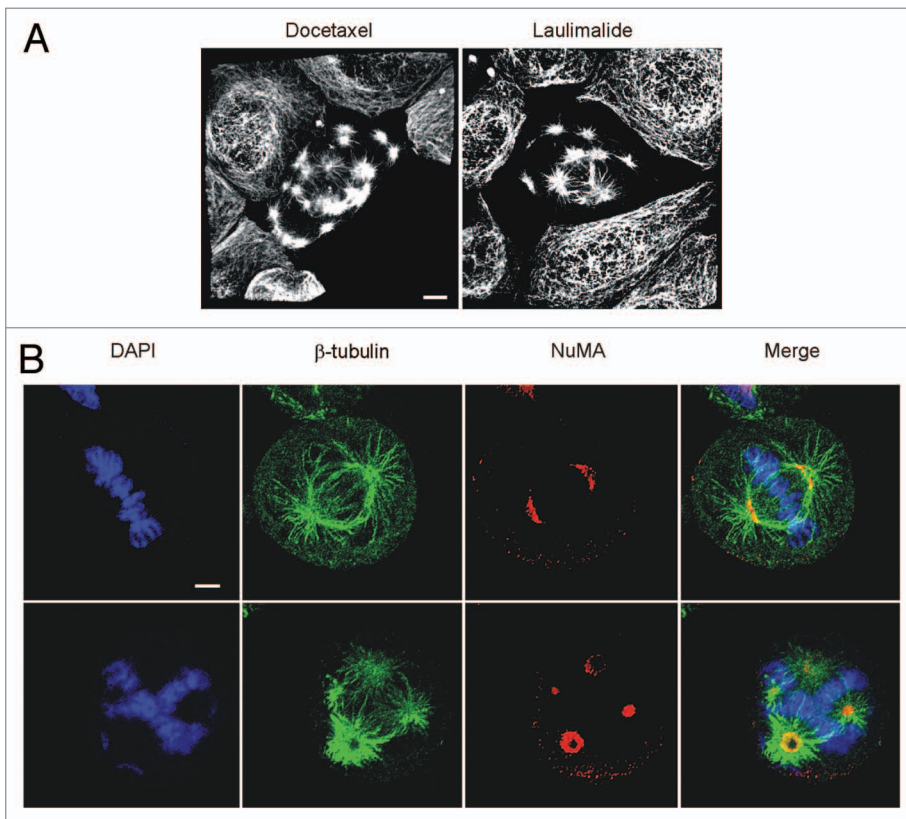


**Figure 4.** Laulimalide induces formation of multiple asters in HeLa cells during early prometaphase, and aberrant pole formation in late prometaphase. (A) Immunofluorescence of  $G_2/M$  synchronized cells incubated with 30 nM docetaxel (left) or 30 nM laulimalide (right) for 2 h. Microtubule asters were detected using a  $\beta$ -tubulin antibody. (B) Immunofluorescence of asynchronous cells incubated with a DMSO control (top) or 30 nM laulimalide (bottom) for 2.5 h showing super-numerary poles marked by the minus-end scaffolding protein NuMA. Tubulin is shown in green, NuMA in red and DAPI in blue. Scale bars represents 10  $\mu\text{m}$  in (A) and 5  $\mu\text{m}$  in (B).

synchronization, only 1% of laulimalide-treated mitotic cells were observed with multiple asters. This increased to 23% upon synchronization, which made it easier to capture this state of assembly. Similar numbers were obtained for docetaxel-treated cells. Electron micrographs confirmed that asters appear at (or very near) the onset of nuclear envelope breakdown (Fig. S2).

The multiplicity of asters represents a highly transient state, as in late prometaphase, fewer organized pole-like structures are observed (Fig. 4B). The MT tethering protein NuMA, shown previously to have a role in organizing asters by crosslinking MT minus ends,<sup>27</sup> was found at all poles but indicated two classes of pole-like structures. One set was very dense, whereas the remaining poles possessed a circular morphology. The M4491 antibody to centrosomal proteins and pericentriolar material<sup>28,29</sup> stained only two poles in laulimalide-treated mature prometaphase cells, showing that centrosome amplification does not occur at low dose, and that the super-numerary poles are acentrosomal/acentriolar (Fig. S3A). Low-dose docetaxel treatment again shows a similar effect, and we also note that  $\gamma$ -tubulin is excluded from the acentrosomal poles (Fig. S3B). These poles are clearly very minimalist in composition, containing as little as NuMA to

focus the MT minus ends. We note that both drugs produced a high percentage of cells with centrosomes that did not separate. This occurred in 25% of the laulimalide and 36% of the docetaxel-treated mitotic cells. It is not surprising that defects in pole formation would affect centrosome separation, as this is a force-dependent process involving the MT network.<sup>30</sup>

Collectively, these data indicate that prior to mitosis, treatment with low concentrations of either stabilizer induces excessive aster formation apparently by altering MT nucleation requirements during the interphase-mitosis transition. Progressing from prophase, the number of asters decline and the remaining asters compete with the intact centrosomal poles for positioning of the chromosomes.

**Effect of laulimalide at metaphase.** The multipolar phenotype induced by laulimalide prevents the formation of a bipolar spindle and thus cells do not progress through metaphase. To determine the effect of laulimalide on cells that had already reached metaphase prior to drug addition, cells were synchronized in G<sub>2</sub>/M using a double thymidine block followed by the addition of MG132 for 1.5 h. MG132 is a proteasome inhibitor that prevents a metaphase-to-anaphase transition by blocking the degradation of securin and cyclin B.<sup>31</sup> At time 0, laulimalide was added to a culture of mCherry tubulin and GFP-CENP-B HeLa cells, and a mitotic cell with an intact chromosomal plate and bipolar spindle was selected for time-lapse observation. The cell maintained its bipolarity over a period of 90 min; however, chromosome congression was lost (Fig. 5). The chromosomes retained an association with the centrosomes, eventually forming a chromosomal array about the spindle pole(s).

To extend these observations, the phenotype of MG132-synchronized cells was quantitated using IIF. After treating with laulimalide for 1 h, 46% of the MG132-synchronized metaphase cells displayed a bipolar spindle and a circular array of chromosomes, in keeping with the time-lapse images (Fig. 6 and Table 1). Washing out MG132 prior to the addition of laulimalide did not significantly alter these results. After treating for two hours, this phenotype represented 67% of the metaphase cells in the presence of MG132, again largely unchanged by inhibitor washout. Previous time-lapse studies showed that metaphase human breast cancer cells treated with low doses of docetaxel resulted in a multipolar phenotype, with spindle poles gradually elongating parallel to the plate until eventual pole fragmentation.<sup>19</sup> As a control for the laulimalide experiment, synchronized cells were therefore treated with docetaxel for up to 2 h and analyzed with IIF. The dominant phenotype was confirmed to be multipolar with extensive centrosome stretching and fragmentation (Fig. 6 and Table 1). Thus, metaphase-synchronized cells treated with laulimalide retain a bipolar phenotype, while docetaxel-treated cells exhibit a fragmented and predominantly multipolar phenotype.

In laulimalide-treated cells, sister chromatids remain associated as chromosomes migrate from the plate to a pole (Fig. 6, arrow). Kinetochores appear normal in electron microscopy (not shown), indicating that kinetochore-MT interactions are dropped upon laulimalide treatment without compromising kinetochore structure. Thus, the mechanism of plate disintegration for the two MT stabilizers are quite different. Pole

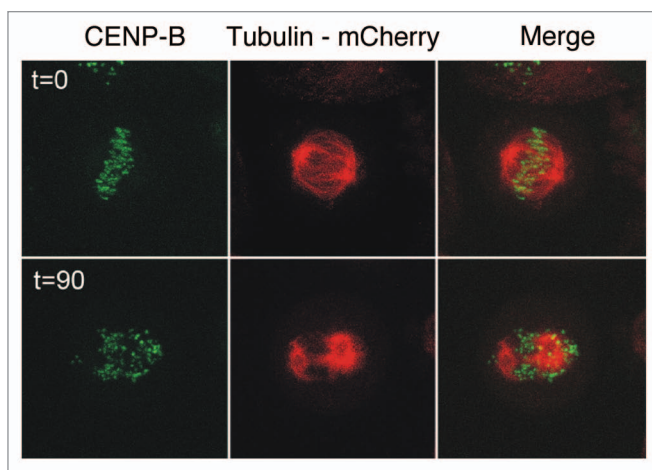


**Figure 5.** Laulimalide scatters chromosomes from the metaphase plate. Live-cell images were obtained for GFP-CENP-B and mCherry tubulin HeLa cells, synchronized in metaphase using MG132 and treated with 30 nM laulimalide. Top: images at  $t = 0$  show a well-formed microtubule spindle array and a metaphase plate. Bottom: images at  $t = 90$  min. show that chromosomes have scattered off the plate, but the two spindle poles remain. CENP-B is shown in green to mark centromeres. Tubulin is shown in red.

fragmentation appears to be a central driver for docetaxel, whereas the reduced fidelity of kinetochore-MT interactions appears more significant for laulimalide. To explore this further, we inspected kinetochore-MT interactions in greater detail. The vehicle- and laulimalide-treated cells had similar pole-to-pole distances, with values of  $14.2 \pm 0.2 \mu\text{m}$  (s.e.m) and  $13.9 \pm 0.3 \mu\text{m}$ , whereas the docetaxel-treated cells had a significantly shorter distance between poles with a value of  $9.8 \pm 0.2 \mu\text{m}$  (Fig. S4). The pole-to-pole distances did not vary over a limited timeframe of 1–2 h, nor did they change upon MG132 washout, highlighting the stability of the effect. The impact of the drugs on the relative tension between sister kinetochores was also measured, focusing on the subset of cells with MTs attached to both kinetochores (Fig. 7). Cells treated with laulimalide exhibited significantly longer distances between sister kinetochores, with a mean value of  $2.64 \pm 0.05 \mu\text{m}$  (s.e.m.) compared with the control and docetaxel-treated cells, having mean values of  $2.14 \pm 0.04 \mu\text{m}$ , and  $2.22 \pm 0.04 \mu\text{m}$  respectively. Additionally, these data show that laulimalide-treated cells preserve or slightly increase the dynamics of kinetochore stretching. The range of kinetochore stretch lengths is  $2 \mu\text{m}$  for laulimalide and  $1.7 \mu\text{m}$  for the untreated control. We see a reduction in the range of stretch lengths for docetaxel-treated cells ( $1.3 \mu\text{m}$ ). These findings suggest that laulimalide induces heightened kinetochore tension, which is unusual for an antimitotic drug.

## Discussion

The identification of MT-stabilizing agents addressing a unique binding site on the MT lattice raises new opportunities to study mechanisms of cell division and may also generate new directions in the development of antimitotic therapies. Ligands

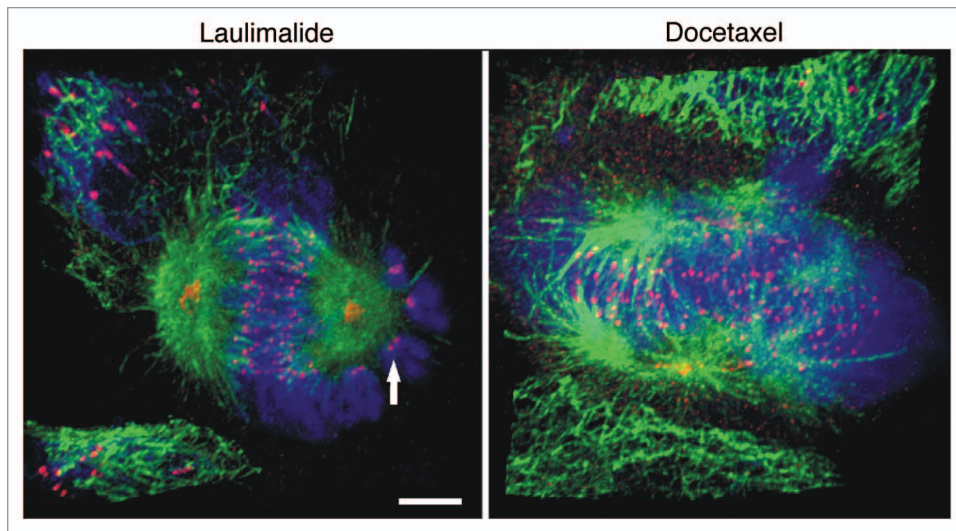


**Figure 6.** Plate disintegration mechanisms differ for laulimalide and docetaxel. Immunofluorescence of HeLa cells synchronized in metaphase and treated with 30 nM laulimalide (left) or 30 nM docetaxel (right) for 1 h. Spindle poles remain under laulimalide treatment, and the arrow shows two sister kinetochores in a chromosome scattered from the plate. Spindle poles disintegrate under docetaxel treatment, and chromosomes decondense prematurely. Tubulin is shown in green, centrosomes and kinetochores in red and DNA in blue. Scale bar represents 5  $\mu\text{m}$ .

targeting tubulin have played a central role in mitotic research, and they continue to do so. In this study, we demonstrate that laulimalide should be viewed as a representative of a distinct class of MT-interfering agents, primarily on the basis of its effects in metaphase and interphase.

There are, however, similarities in the phenotype displayed by docetaxel and laulimalide, in keeping with the initial studies conducted at high drug concentrations.<sup>4,7,16</sup> Both drugs interfere with the proper formation of the mitotic spindle, through the generation of multiple MT asters at or near the onset of nuclear envelope breakdown. The formation of multiple asters at this stage appears to be a common property of all types of microtubule targeting agents, including stabilizers, destabilizers and microtubule-modulating drugs like EM011.<sup>32-34</sup>

Precisely how MT asters are formed is not well understood. Several studies suggest these asters arise from increased polymerization of MT states in the cytoplasm.<sup>35,36</sup> Alternatively, Hornick et al. propose that multiple MT aster formation is driven by a redistribution of pre-assembled microtubules from the centrosomes to the cell cortex.<sup>32</sup> Our data suggest that both laulimalide and docetaxel drive MT assembly and lower the barrier for effective nucleation of minus-end MTs; this is supported by the formation of multiple acentrosomal poles without centrosomal proteins or pericentriolar material. Potentially NuMA may be all that is required for stabilizing these poles. When considering spindle poles from a thermodynamic standpoint, as an equilibrium involving many-protein interactions, it is sensible that greater stability in a key structural unit (MTs) would require a less robust organizing center. On this basis, at higher drug concentrations one could expect the dominance or persistence of such poles. This is in keeping with the initial investigations of laulimalide.<sup>4,7,16</sup>

The formation of supernumerary poles may be viewed as a competitive element in the establishment of kinetochore-MT interactions, which is a model recently proposed by Sakaushi et al.<sup>37</sup> Centrosomal spindle poles are still present but they are not able to restrict aberrant poles from attempts to organize the chromosomal mass. Although this effect is similar with the two stabilizers, the frequency of the multipolar phenotype is quite different. There exists a stronger bias toward a multipolar spindle for docetaxel even in asynchronous cell populations (not shown), which became much more evident in a cell population synchronized at metaphase (Table 1). It appears that the generation of acentrosomal poles is more potent using docetaxel as opposed to laulimalide, or that nascent centrosomal poles in laulimalide-treated cells are able to

compete more effectively with the MT asters formed at nuclear envelope breakdown. This is supported by the centrosome fragmentation that we observed when metaphase cells were treated with docetaxel and the absence of centrosome fragmentation using laulimalide.

Our observations are in keeping with the variability in spindle pole formation observed for a variety of MT-acting agents.<sup>19,33</sup> The outcome of premature aster formation ranges from mild effects on the spindle as seen with epothilone A,<sup>37</sup> where the bipolar spindle is retained, to severe as seen with paclitaxel,<sup>12</sup> epothilone B<sup>12,37</sup> and docetaxel,<sup>19</sup> where multipolar spindles are formed with inhibition of pole separation at higher doses. When compared with these other MT-stabilizing agents, laulimalide favors an intermediate spindle phenotype, as long as the drug is present before nuclear envelope breakdown.

A central finding of our study is that laulimalide increases kinetochore tension in a preformed spindle. This is unexpected and intriguing, as reduced tension is a hallmark of microtubule stabilizers like paclitaxel, presumably deriving from reduced MT dynamics.<sup>10,38</sup> We do not observe a statistically significant reduction in average interkinetochore spacing for docetaxel-treated cells relative to the control, which may simply mean that docetaxel is not as potent as paclitaxel in reducing tension. However, the reduced range of stretch in docetaxel-treated cells does suggest reduced centromere dynamics, in keeping with paclitaxel,<sup>38</sup> which may ultimately be a more direct measure of reduced MT dynamics.

The basis for the increase in kinetochore tension under laulimalide treatment is currently unclear. If laulimalide reduces MT dynamics in a manner similar to peloruside A (a ligand that binds to the same site),<sup>39</sup> it raises the interesting idea that tension reduction may not require reduced plus-end MT dynamics.

**Table 1.** Influence of MT stabilizers on metaphase morphology

Phenotype	Drug treatment*		Drug treatment (MG-132 washout)	
	1 h	2 h	1 h	2 h
Bipolar <sup>a</sup>	27/11	5/1	31/20	10/0
Bipolar <sup>b</sup>	46/7	67/6	41/13	76/8
Multipolar <sup>c</sup>	26/82	28/93	29/67	15/92

\*Laulimalide/docetaxel. Number in percentages of total cell population, based on 100 cells. <sup>a</sup>Intact chromosome plate. <sup>b</sup>Scattering of chromosomes off the plate. <sup>c</sup>Intact or fragmented chromosome plate.

Kinetochores may correlate better with spindle pole integrity by promoting poleward forces more efficiently, perhaps with intact spindle poles supporting a more effective minus-end disassembly and poleward flux.<sup>40</sup> The functional impact of increased tension under the action of laulimalide appears to be dropped kinetochore-MT interactions, which leads to the scattering of chromatid pairs to one or the other pole. Migration of pairs distinguishes the effect from “cohesion fatigue” that occurs with prolonged treatment with MG132, in which chromatid separation occurs in a similarly unscheduled fashion.<sup>41</sup> Dropped kinetochore-MT interactions happen prior to the onset of fatigue, in under 90 min (Fig. 5).

Dropped interactions may at first seem inconsistent with a heightened state of kinetochore stretch or tension, but only if kinetochore stretch is taken to mean stronger, more viable interactions between kinetochores and MTs. This is not likely to be the case. Dropped connections can either arise from a drug-induced weakening of kinetochore-MT interactions, or strained interactions where poleward force generation exceeds an overall stability threshold at some element in the junction. When considering the first possibility, a weaker interaction state is not consistent with our data, as we see abnormally high kinetochore stretching. Further, although destabilization could be an outcome of perturbed MT dynamics by the drug, activating the spindle assembly checkpoint and releasing MTs from the kinetochore,<sup>10,42</sup> presumably this would sever all kinetochore-MT connections. Rather, we observe a random shearing that leaves one MT connection to unseparated chromatid pairs.

The second possibility, that of excessive force generation and connection failure has support from existing mechanochemical models of the kinetochore-MT interaction. Poleward flux and dynamic kinetochore-MT attachments maintain a tensioned state in metaphase.<sup>43</sup> Balancing the MT dynamics at the plus end and preventing the attachment machinery from “parking” the kinetochore on the spindle MTs creates a state where mechanical force can be effectively managed. The heightened kinetochore tension that we observe followed by random releasing of only one of two contacts is most consistent with a perturbed mechanism of force regulation. Precisely how laulimalide unbalances this so-called “slip-clutch” mechanism<sup>43</sup> while docetaxel does not is unclear, but measurements of poleward flux based on microtubule treadmilling and MT binding strength of key kinetochore proteins (e.g., Ndc80) will be effective in testing this idea. For example, if laulimalide generates an MT state where Ndc80 binds

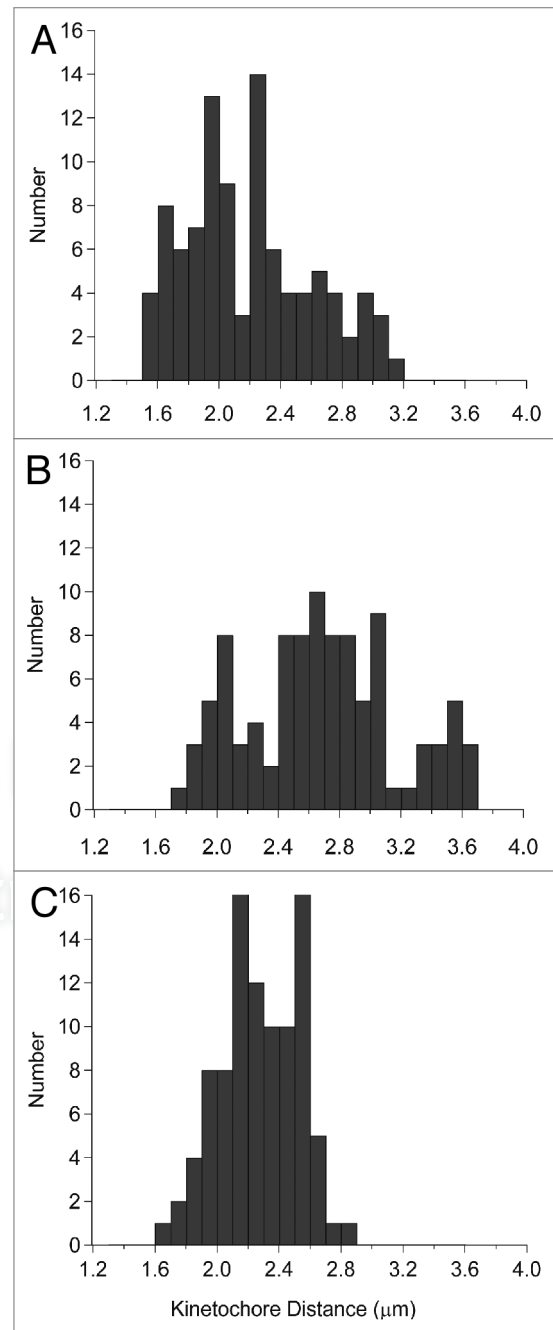


**Figure 7.** Laulimalide treatment in metaphase produces increased kinetochore separation. Distances were measured from 100 kinetochore pairs in HeLa cells treated with (A) DMSO as a control (B) 30 nM laulimalide or (C) 30 nM docetaxel for 1–2 h. Calculation of distances were made on MG132-synchronized cells, using M4491 stain to mark kinetochores.

more effectively to the MT lattice compared with docetaxel, this could increase friction and produce a “sticky” clutch that permits the accumulation of excessive force and ultimate failure in the attachment. The current study clearly highlights the utility of laulimalide, together with taxoids, as useful molecular probes for further investigations of the relationships between MT dynamics, kinetochore tension and the spindle checkpoint.

The distinct nature of the MT-stabilizing site represented by laulimalide may supply a unifying concept for both the similarities and differences observed in this study. As laulimalide and docetaxel have been found to stabilize MTs indistinguishably in simple biochemical preparations, it is not surprising that aspects of the cellular response are similar—the formation of multiple asters at nuclear envelope breakdown and the increased acetylation of interphase MTs. The differences that we observe in interphase MT bundling, centrosomal pole fragmentation and the integrity of kinetochore-MT interactions may represent the inhibition of MT-binding proteins with a role in regulating these disparate functions. The laulimalide site is exposed in a way not seen with the taxoid site—it is accessible from the outside of the lattice in a region viewed as critical for establishing control over protofilament number and plus-end tracking proteins (Fig. S5).<sup>44,45</sup> Testing the idea of laulimalide as a direct inhibitor of lattice regulators awaits further proteomic-level analyses.

Our findings confirm that laulimalide represents a class of MT-stabilizer that are sufficiently distinct from the taxoids and their mimetics to warrant further study as a molecular probe and potentially also as a new category of antimitotic therapy.

## Materials and Methods

**Cell culture.** HeLa cells obtained from the American Type Culture Collection were cultured in DMEM medium supplemented with 10% FBS (Invitrogen, 11960–044) and 2mM L-glutamine (Invitrogen, 25030–081) at 37°C in 5% CO<sub>2</sub>. For live-cell imaging, stably transfected HeLa cells including mCherry-tubulin with GFP-H2B and mCherry with CENP-B-GFP were used. The cell lines were either synchronized using a double thymidine block and released to observe G<sub>2</sub>/M events, or at metaphase using a double thymidine block and released into fresh media containing 12.5 μM MG132 (VWR, 80053–196) for 1.5 h.<sup>46</sup> The double thymidine block was conducted by treating HeLa cells with 2 mM thymidine in media for 16 h, followed by an 8 h release. This was repeated a second time. After the final 8 h release, mitotic cells (as observed under light microscopy) began to appear. These were either trypsinized for flow cytometry analysis, treated with laulimalide or docetaxel, or synchronized in metaphase using 12.5 μM of MG132 for 1 or 2 h followed by laulimalide or docetaxel treatment.

**Antibodies.** MTs were detected using a mouse monoclonal β-tubulin antibody at a 1/50 dilution that was developed by Michael Klymkowsky and obtained from the Developmental Studies Hybridoma Bank developed under the auspices of the NICHD and maintained by the University of Iowa, Department of Biology. Centrosomes and kinetochores were detected using the human autoimmune serum M4491 at a 1/3,000 dilution, obtained from the serum bank of the Advanced Diagnostic Laboratory at the University of Calgary. Characterization of this serum has been reported previously.<sup>28,29</sup> NuMA was detected using a human serum containing autoantibodies to this protein as previously described, at a 1/500 dilution.<sup>47</sup> Acetylated microtubules were detected using a mouse anti-acetylated tubulin antibody (Sigma, T6793) at a 1/1,000 dilution. Gamma-tubulin was

detected using a rabbit polyclonal γ-tubulin antibody (Sigma, T5192) at a 1/1,000 dilution. Mouse antibodies were detected using anti-mouse secondary antibodies conjugated to Alexa 488 (Invitrogen, A11001), human antibodies were detected using anti-human secondary antibodies conjugated to Cy3 (Jackson ImmunoResearch, 109–166–064) and rabbit antibodies were detected using anti-rabbit secondary antibodies conjugated to Alexa 488 (Invitrogen, A11008), all at a 1/200 dilution.

**Immunofluorescence.** HeLa cells were plated on glass coverslips and allowed to adhere for 1 d before addition of laulimalide or docetaxel at the indicated concentrations. After drug addition, cells were fixed in cold methanol for 15 min and then rinsed and placed in PBS. Fixed cells were washed with PBS and incubated with the primary antibody for 30 min. After several washes in PBS, the samples were incubated for 30 min with the appropriate secondary antibody. The samples were then washed in PBS and counterstained with DAPI (Sigma, D8417) followed by another PBS wash. The cells were then mounted on a glass slide using 90% glycerol containing paraphenylenediamine (VWR, CAAA15680–30). Cells were visualized using a Zeiss 710 LSM series confocal microscope with a 63 x 1.4NA Oil DIC Plan-Apochromat lens or a Zeiss Axiovert 200 MOT inverted fluorescence microscope. Z-stacks were performed using a 0.3 μm step size. Deconvolution was performed using Huygens Essential from SVI (www.svi.nl). Images were processed using Photoshop version 9.0.2 (Adobe Systems) and Imaris (Bitplane) software. Kinetochore distance and pole-to-pole distance measurements were performed using Imaris software (Bitplane).

**Live-cell imaging.** HeLa mCherry H2B-GFP and HeLa mCherry CENP-B-GFP stable cell lines were synchronized using a double thymidine block and released to observe G<sub>2</sub>/M events, or synchronized in metaphase using MG132. HeLa cells stably expressing the various fluorescent-protein-tagged proteins were plated onto 35 mm glass bottom dishes (FluoroDish, World Precision Instruments). Live-cell imaging was performed with the Ultraview ERS Rapid confocal imager (PerkinElmer) mounted on a Zeiss Axiovert 200M inverted microscope with an EMCCD Camera (Hamamatsu). Dishes containing the cells were placed onto the microscope within an environmental control chamber, maintaining the temperature at 37°C. Laulimalide or docetaxel were added directly to the dishes at the indicated times. The cells were imaged every 1 min, and a stack of images with a Z step size of 1 μm were collected. All images were collected with a 63x plan-apochromatic lens (NA 1.4) with appropriate filter configurations for different fluorescent protein tags (EGFP: excitation at 488 nm and emission filter of 500–550 nm; mCherry: excitation at 561 nm and emission filter of 580–700 nm). The data was analyzed with UltraVIEWERS software (PerkinElmer) and converted into QuickTime (Apple) movie files. The time-lapse images were collected and illustrated using Photoshop.

**Flow cytometry.** HeLa cells (1 x 10<sup>6</sup>) were treated with either DMSO for 5 h, laulimalide for 2.5 h or laulimalide for 5 h. The cells were then trypsinized and placed in a centrifugation tube with fresh media. The cells were then washed with PBS followed by the addition of 95% cold ethanol and stored at 4°C for 24

h. The cells were then centrifuged for a final time in PBS and resuspended in propidium iodide (PI) staining buffer (50  $\mu\text{g}/\text{ml}$  PI, 0.1% Triton X 100, 0.2 mg DNase free RNase A in PBS) for 30 min. The cell cycle distribution was analyzed on a FACS flow cytometer. Propidium iodide intensity was plotted vs. the number of counts using FlowJo software (Tree star). The percentage of cells in each phase of the cell cycle was analyzed using ModfitLT 3.0 (Verity House Software).

**Electron microscopy.** HeLa cells treated with 30 nM laulimalide and 30 nM docetaxel for 2.5 h were fixed in 3% glutaraldehyde in Millonig's phosphate buffer for 1 h at room temperature. Post-fixation was in 2%  $\text{OsO}_4$  for 20 min. The cells were dehydrated in ethanol, and then infiltrated with Polybed 812 resin (Polysciences, #08792-1). Polymerization was performed at 37°C for 24 h. Silver-gray sections were cut with an ultramicrotome (Leica) equipped with a diamond knife, and sections were stained with uranyl acetate and lead citrate and examined in an electron microscope (H-7000:Hitachi).

**Materials.** Docetaxel was provided by Alberta Health Services, Tom Baker Cancer Institute. Docetaxel was dissolved in DMSO at a concentration of 5 mM and stored at -80°C. Laulimalide was kindly provided by Dr. Dan Sackett (National Institutes of Health) dissolved in DMSO at a concentration of 5 mM and stored at -80°C. MG132 (VWR) was used at a final concentration of 12.5  $\mu\text{M}$ . Thymidine (Sigma, T1895) was used at a final concentration of 2 mM. The GFP-histone H2B plasmid

was a kind gift from Dr. G. Wahl (Salk Institute for Biological Studies). The mCherry tubulin and mCherry histone H2B plasmids were kind gifts from Dr. Michael Davidson (National High Magnetic Field Laboratory, Florida State University). The GFP-CENP-B plasmid was a kind gift from Dr. Kevin Sullivan (National University of Ireland).

#### Disclosure of Potential Conflicts of Interest

No potential conflicts of interest were disclosed.

#### Acknowledgments

We thank Dan L. Sackett (National Institute of Child Health and Human Development, NIH) for the provision of laulimalide and his helpful comments on the manuscript. We thank Dr. Xuejun Sun and the Cross Cancer Institute Cell Imaging Facility for assistance with the microscopy described in this work. The work was supported by Alberta Innovates—Health Solutions and the Alberta Cancer Foundation (201000620, G.K.C. and D.C.S.). J.B.R. acknowledges funding support from NSERC. G.K.C. acknowledges funding support from NSERC. D.C.S. acknowledges the additional support of the Canada Research Chair program.

#### Supplemental Materials

Supplemental materials may be found here: [www.landesbioscience.com/journals/cc/article/21411](http://www.landesbioscience.com/journals/cc/article/21411)

#### References

- Bennett MJ, Barakat K, Huzil JT, Tuszyński J, Schriemer DC. Discovery and characterization of the laulimalide-microtubule binding mode by mass shift perturbation mapping. *Chem Biol* 2010; 17:725-34; PMID:20659685; <http://dx.doi.org/10.1016/j.chembiol.2010.05.019>.
- Kanakkanthara A, Wilmes A, O'Brate A, Escuin D, Chan A, Gyrezi A, et al. Peloruside- and laulimalide-resistant human ovarian carcinoma cells have  $\beta\text{I}$ -tubulin mutations and altered expression of  $\beta\text{II}$ - and  $\beta\text{III}$ -tubulin isotypes. *Mol Cancer Ther* 2011; 10:1419-29; PMID:21653684; <http://dx.doi.org/10.1158/1535-7163.MCT-10-1057>.
- Begaye A, Trostel S, Zhao Z, Taylor RE, Schriemer DC, Sackett DL. Mutations in the  $\beta$ -tubulin binding site for peloruside A confer resistance by targeting a cleft significant in side chain binding. *Cell Cycle* 2011; 10:3387-96; PMID:21926482; <http://dx.doi.org/10.4161/cc.10.19.17706>.
- Mooberry SL, Tien G, Hernandez AH, Plubrukarn A, Davidson BS. Laulimalide and isolaulimalide, new paclitaxel-like microtubule-stabilizing agents. *Cancer Res* 1999; 59:653-60; PMID:9973214.
- Pryor DE, O'Brate A, Bilcer G, Díaz JF, Wang Y, Wang Y, et al. The microtubule stabilizing agent laulimalide does not bind in the taxoid site, kills cells resistant to paclitaxel and epothilones, and may not require its epoxide moiety for activity. *Biochemistry* 2002; 41:9109-15; PMID:12119025; <http://dx.doi.org/10.1021/bi020211b>.
- Hamel E, Day BW, Miller JH, Jung MK, Northcote PT, Ghosh AK, et al. Synergistic effects of peloruside A and laulimalide with taxoid site drugs, but not with each other, on tubulin assembly. *Mol Pharmacol* 2006; 70:1555-64; PMID:16887932; <http://dx.doi.org/10.1124/mol.106.027847>.
- Liu J, Towle MJ, Cheng H, Saxton P, Reardon C, Wu J, et al. In vitro and in vivo anticancer activities of synthetic (-)-laulimalide, a marine natural product microtubule stabilizing agent. *Anticancer Res* 2007; 27(3B):1509-18; PMID:17595769.
- Yvon AM, Wadsworth P, Jordan MA. Taxol suppresses dynamics of individual microtubules in living human tumor cells. *Mol Biol Cell* 1999; 10:947-59; PMID:10198049.
- Jordan MA, Toso RJ, Thrower D, Wilson L. Mechanism of mitotic block and inhibition of cell proliferation by taxol at low concentrations. *Proc Natl Acad Sci USA* 1993; 90:9552-6; PMID:8105478; <http://dx.doi.org/10.1073/pnas.90.20.9552>.
- Waters JC, Chen RH, Murray AW, Salmon ED. Localization of Mad2 to kinetochores depends on microtubule attachment, not tension. *J Cell Biol* 1998; 141:1181-91; PMID:9606210; <http://dx.doi.org/10.1083/jcb.141.5.1181>.
- Andreassen PR, Martineau SN, Margolis RL. Chemical induction of mitotic checkpoint override in mammalian cells results in aneuploidy following a transient tetraploid state. *Mutat Res* 1996; 372:181-94; PMID:9015137; [http://dx.doi.org/10.1016/S0027-5107\(96\)00138-8](http://dx.doi.org/10.1016/S0027-5107(96)00138-8).
- Chen JG, Horwitz SB. Differential mitotic responses to microtubule-stabilizing and -destabilizing drugs. *Cancer Res* 2002; 62:1935-8; PMID:11929805.
- Brito DA, Yang Z, Rieder CL. Microtubules do not promote mitotic slippage when the spindle assembly checkpoint cannot be satisfied. *J Cell Biol* 2008; 182:623-9; PMID:18710927; <http://dx.doi.org/10.1083/jcb.200805072>.
- Sherline P, Mascardo R. Epidermal growth factor-induced centrosomal separation: mechanism and relationship to mitogenesis. *J Cell Biol* 1982; 95:316-22; PMID:6982901; <http://dx.doi.org/10.1083/jcb.95.1.316>.
- Vader G, Crujnsen CW, van Harn T, Vromans MJ, Medema RH, Lens SM. The chromosomal passenger complex controls spindle checkpoint function independent from its role in correcting microtubule kinetochore interactions. *Mol Biol Cell* 2007; 18:4553-64; PMID:17699588; <http://dx.doi.org/10.1091/mbc.E07-04-0328>.
- Mooberry SL, Randall-Hlubek DA, Leal RM, Hegde SG, Hubbard RD, Zhang L, et al. Microtubule-stabilizing agents based on designed laulimalide analogues. *Proc Natl Acad Sci USA* 2004; 101:8803-8; PMID:15161976; <http://dx.doi.org/10.1073/pnas.0402759101>.
- Torres K, Horwitz SB. Mechanisms of Taxol-induced cell death are concentration dependent. *Cancer Res* 1998; 58:3620-6; PMID:9721870.
- Paoletti A, Giocanti N, Favaudon V, Bornens M. Pulse treatment of interphasic HeLa cells with nanomolar doses of docetaxel affects centrosome organization and leads to catastrophic exit of mitosis. *J Cell Sci* 1997; 110:2403-15; PMID:9410879.
- Sakaushi S, Nishida K, Minamikawa H, Fukada T, Oka S, Sugimoto K. Live imaging of spindle pole disorganization in docetaxel-treated multicolor cells. *Biochem Biophys Res Commun* 2007; 357:655-60; PMID:17448447; <http://dx.doi.org/10.1016/j.bbrc.2007.03.205>.
- Morse DL, Gray H, Payne CM, Gillies RJ. Docetaxel induces cell death through mitotic catastrophe in human breast cancer cells. *Mol Cancer Ther* 2005; 4:1495-504; PMID:16227398; <http://dx.doi.org/10.1158/1535-7163.MCT-05-0130>.
- Schiff PB, Horwitz SB. Taxol stabilizes microtubules in mouse fibroblast cells. *Proc Natl Acad Sci USA* 1980; 77:1561-5; PMID:6103535; <http://dx.doi.org/10.1073/pnas.77.3.1561>.
- Kung AL, Sherwood SW, Schimke RT. Cell line-specific differences in the control of cell cycle progression in the absence of mitosis. *Proc Natl Acad Sci USA* 1990; 87:9553-7; PMID:2263610; <http://dx.doi.org/10.1073/pnas.87.24.9553>.

23. Jordan MA, Wendell K, Gardiner S, Derry WB, Copp H, Wilson L. Mitotic block induced in HeLa cells by low concentrations of paclitaxel (Taxol) results in abnormal mitotic exit and apoptotic cell death. *Cancer Res* 1996; 56:816-25; PMID:8631019.
24. Lawo S, Bashkurov M, Mullin M, Ferreria MG, Kittler R, Habermann B, et al. HAUS, the 8-subunit human Augmin complex, regulates centrosome and spindle integrity. *Curr Biol* 2009; 19:816-26; PMID:19427217; <http://dx.doi.org/10.1016/j.cub.2009.04.033>.
25. Wloga D, Gaertig J. Posttranslational modifications of microtubules. *J Cell Sci* 2010; 123:3447-55; PMID:20930140; <http://dx.doi.org/10.1242/jcs.063727>.
26. Piperno G, LeDizet M, Chang XJ. Microtubules containing acetylated alpha-tubulin in mammalian cells in culture. *J Cell Biol* 1987; 104:289-302; PMID:2879846; <http://dx.doi.org/10.1083/jcb.104.2.289>.
27. Khodjakov A, Cole RW, Oakley BR, Rieder CL. Centrosome-independent mitotic spindle formation in vertebrates. *Curr Biol* 2000; 10:59-67; PMID:10662665; [http://dx.doi.org/10.1016/S0960-9822\(99\)00276-6](http://dx.doi.org/10.1016/S0960-9822(99)00276-6).
28. Mack GJ, Rees J, Sandblom O, Balczon R, Fritzler MJ, Rattner JB. Autoantibodies to a group of centrosomal proteins in human autoimmune sera reactive with the centrosome. *Arthritis Rheum* 1998; 41:551-8; PMID:9506584; [http://dx.doi.org/10.1002/1529-0131\(199803\)41:3<551::AID-ART22>3.0.CO;2-X](http://dx.doi.org/10.1002/1529-0131(199803)41:3<551::AID-ART22>3.0.CO;2-X).
29. Ou Y, Rattner JB. A subset of centrosomal proteins are arranged in a tubular conformation that is reproduced during centrosome duplication. *Cell Motil Cytoskeleton* 2000; 47:13-24; PMID:11002307; [http://dx.doi.org/10.1002/1097-0169\(200009\)47:1<13::AID-CM2>3.0.CO;2-C](http://dx.doi.org/10.1002/1097-0169(200009)47:1<13::AID-CM2>3.0.CO;2-C).
30. Mardin BR, Schiebel E. Breaking the ties that bind: new advances in centrosome biology. *J Cell Biol* 2012; 197:11-8; PMID:22472437; <http://dx.doi.org/10.1083/jcb.201108006>.
31. Lee DH, Goldberg AL. Proteasome inhibitors: valuable new tools for cell biologists. *Trends Cell Biol* 1998; 8:397-403; PMID:9789328; [http://dx.doi.org/10.1016/S0962-8924\(98\)01346-4](http://dx.doi.org/10.1016/S0962-8924(98)01346-4).
32. Hornick JE, Bader JR, Tribble EK, Trimble K, Breunig JS, Halpin ES, et al. Live-cell analysis of mitotic spindle formation in taxol-treated cells. *Cell Motil Cytoskeleton* 2008; 65:595-613; PMID:18481305; <http://dx.doi.org/10.1002/cm.20283>.
33. Sakaushi S, Senda-Murata K, Oka S, Sugimoto K. Visualization of aberrant perinuclear microtubule aster organization by microtubule-destabilizing agents. *Biosci Biotechnol Biochem* 2009; 73:1192-6; PMID:19420700; <http://dx.doi.org/10.1271/bbb.80754>.
34. Karna P, Rida PC, Pannu V, Gupta KK, Dalton WB, Joshi H, et al. A novel microtubule-modulating nospainoid triggers apoptosis by inducing spindle multipolarity via centrosome amplification and declustering. *Cell Death Differ* 2011; 18:632-44; PMID:21052096; <http://dx.doi.org/10.1038/cdd.2010.133>.
35. Verde F, Berrez JM, Antony C, Karsenti E. Taxol-induced microtubule asters in mitotic extracts of *Xenopus* eggs: requirement for phosphorylated factors and cytoplasmic dynein. *J Cell Biol* 1991; 112:1177-87; PMID:1671864; <http://dx.doi.org/10.1083/jcb.112.6.1177>.
36. De Brabander M, Geuens G, Nuydens R, Willebrords R, De Mey J. Taxol induces the assembly of free microtubules in living cells and blocks the organizing capacity of the centrosomes and kinetochores. *Proc Natl Acad Sci USA* 1981; 78:5608-12; PMID:6117858; <http://dx.doi.org/10.1073/pnas.78.9.5608>.
37. Sakaushi S, Nishida K, Fukada T, Senda-Murata K, Oka S, Sugimoto K. Differential responses of mitotic spindle pole formation to microtubule-stabilizing agents epothilones A and B at low concentrations. *Cell Cycle* 2008; 7:477-83; PMID:18235240; <http://dx.doi.org/10.4161/cc.7.4.5313>.
38. Kelling J, Sullivan K, Wilson L, Jordan MA. Suppression of centromere dynamics by Taxol in living osteosarcoma cells. *Cancer Res* 2003; 63:2794-801; PMID:12782584.
39. Chan A, Andreae PM, Northcote PT, Miller JH. Peloruside A inhibits microtubule dynamics in a breast cancer cell line MCF7. *Invest New Drugs* 2011; 29:615-26; PMID:20169398; <http://dx.doi.org/10.1007/s10637-010-9398-2>.
40. Waters JC, Mitchison TJ, Rieder CL, Salmon ED. The kinetochore microtubule minus-end disassembly associated with poleward flux produces a force that can do work. *Mol Biol Cell* 1996; 7:1547-58; PMID:8898361.
41. Daum JR, Potapova TA, Sivakumar S, Daniel JJ, Flynn JN, Rankin S, et al. Cohesion fatigue induces chromatid separation in cells delayed at metaphase. *Curr Biol* 2011; 21:1018-24; PMID:21658943; <http://dx.doi.org/10.1016/j.cub.2011.05.032>.
42. Nicklas RB, Ward SC. Elements of error correction in mitosis: microtubule capture, release, and tension. *J Cell Biol* 1994; 126:1241-53; PMID:8063861; <http://dx.doi.org/10.1083/jcb.126.5.1241>.
43. Maddox P, Straight A, Coughlin P, Mitchison TJ, Salmon ED. Direct observation of microtubule dynamics at kinetochores in *Xenopus* extract spindles: implications for spindle mechanics. *J Cell Biol* 2003; 162:377-82; PMID:12900391; <http://dx.doi.org/10.1083/jcb.200301088>.
44. Aylett CH, Löwe J, Amos LA. New insights into the mechanisms of cytomotive actin and tubulin filaments. *Int Rev Cell Mol Biol* 2011; 292:1-71; PMID:22078958; <http://dx.doi.org/10.1016/B978-0-12-386033-0.00001-3>.
45. Fourniol FJ, Sindelar CV, Amigues B, Clare DK, Thomas G, Perderiset M, et al. Template-free 13-prot filament microtubule-MAP assembly visualized at 8 Å resolution. *J Cell Biol* 2010; 191:463-70; PMID:20974813; <http://dx.doi.org/10.1083/jcb.201007081>.
46. Famulski JK, Chan GK. Aurora B kinase-dependent recruitment of hZW10 and hROD to tensionless kinetochores. *Curr Biol* 2007; 17:2143-9; PMID:18065224; <http://dx.doi.org/10.1016/j.cub.2007.11.037>.
47. Whitehead CM, Winkfein RJ, Fritzler MJ, Rattner JB. The spindle kinesin-like protein HsEg5 is an autoantigen in systemic lupus erythematosus. *Arthritis Rheum* 1996; 39:1635-42; PMID:8843853; <http://dx.doi.org/10.1002/art.1780391005>.